Annals of Diagnostic Pathology 47 (2020) 151557

Contents lists available at ScienceDirect

Annals of Diagnostic Pathology

journal homepage: www.elsevier.com/locate/anndiagpath

CRABP2 and FABP5 expression levels in diseased and normal pancreas

Christine S. Hughes[a], Jo-Anne ChinAleong[b], Hemant M. Kocher[a,b,*]

[a] Centre for Tumour Biology, Barts Cancer Institute - a CR-UK Centre of Excellence, Queen Mary University of London, Charterhouse Square, EC1M 6BQ London, UK
[b] Barts and the London HPB Centre, Department of Surgery and Pathology, Barts Health NHS Trust, The Royal London Hospital, London E1 1BB, UK

ARTICLE INFO

Keywords:
Immunoflourescence
Pancreas
Cancer
Retinoids
Atra

ABSTRACT

Recently, stromal targeting, by agents such as *All trans* retinoic acid (ATRA), has been regarded as a promising avenue for the treatment of pancreatic ductal adenocarcinoma (PDAC). The intra-cellular transportation of ATRA to the nuclear receptors is performed by either: fatty acid binding protein 5 (FABP5) or cellular retinoic acid binding protein 2 (CRABP2), dictating the transcription of downstream genes and, thus, eventual cell phenotype. Here, we explored the levels of each protein, in pancreatic tissues of patients presenting with a range of pancreatic diseases (pancreatic ductal adenocarcinoma (PDAC), chronic pancreatitis (CP), cholangiocarcinoma (CC)).

We demonstrate that there is a significantly lower CRABP2 and FABP5 expression in activated fibroblasts or pancreatic stellate cells (PSC) in PDAC, as well as other diseased pancreas as in CC and CP, versus quiescent fibroblasts. The quiescent fibroblasts consistently show a pattern of high FABP5:CRABP2 ratio, whereas PSC in all non-PDAC tissues showed a low FABP5:CRABP2 ratio. PSC in PDAC patients had a range of FABP5:CRABP2 ratios (high, even and low).

There was a lower CRABP2 expression in cancerous epithelial cells (PDAC) versus normal epithelial cells. This is also present in other disease states (CP, CC). Contrasting to the patterns seen for fibroblasts, the FABP5 expression in PDAC epithelial cells matched that of the normal epithelial cells. However, the normal epithelial cells had a high FABP5:CRABP2 ratio, compared to the PDAC epithelial cells. These ratios may have correlation with tumor progression, and overall survival. These findings could be confirmed in in vitro cell lysates. CRABP2 and FABP5 levels and ratios could serve as valuable biomarkers.

1. Introduction

Patients with pancreatic ductal adenocarcinoma (PDAC) lack pancreatic and biliary secretions, which leads to a deficiency of fat-soluble vitamins, such as vitamin A (retinol). Pancreatic stellate cells (PSCs) lose their retinol stores to trans-differentiate into activated (myo-)fibroblasts, also known as cancer-associated fibroblasts (CAFs), which in turn are responsible for the desmoplastic reaction in PDAC [1]. Chronic pancreatitis as well as other pancreatic disorders also affect PSC behaviour. *All trans*-retinoic acid (ATRA) restores retinol depots, reverting PSCs to quiescent state [2]. Thus RA transport is important to pathophysiology of the pancreas.

ATRA is transported from the cytosol to the nucleus via fatty acid binding protein 5 (FABP5) and cellular retinoic acid binding protein 2 (CRABP2), leading to binding with the transcription factors peroxisome proliferator-associated receptors (PPAR) and retinoic acid receptors (RAR), respectively [3]. These transcription factors both heterodimerize with rexinoid X receptors (RXR), and bind to their respective regulatory elements, to alter transcriptional activity leading to enhanced differentiation and apoptosis (via CRABP2) versus cell survival (via FABP5) [3]. In this work, we sought to elucidate the differential expression of FABP5 and CRABP2 in pancreatic cancer cells as well as PSC to understand the RA patho-physiology in various pancreatic disorders.

2. Methods

2.1. Tissue micro-array

Tissue microarrays (TMAs) were constructed containing 159 1-mm-diameter core from formalin fixed paraffin-embedded (FFPE) blocks belonging to 53 patients (each patient represented by three cores) with a variety of pancreatic diseases using Tissue Arrayer Minicore® 3 (Alphelys) with prior Research Ethics Committee approval (East

* Corresponding author at: Centre for Tumour Biology, Barts Cancer Institute - a CR-UK Centre of Excellence, Queen Mary University of London, Charterhouse Square, EC1M 6BQ London, UK.
E-mail address: h.kocher@qmul.ac.uk (H.M. Kocher).

https://doi.org/10.1016/j.anndiagpath.2020.151557

London & the City REC3 07/H0705/87) as described previously [4]. 4 μm thick sections were cut and evaluated for CRABP2 and FABP5 expression. Some cores had to be excluded from analysis due to inadequate representative pancreatic or suboptimal staining. As a result, 110 (69%) or 99 (62%) cores could be used in the final analysis, for the scoring of FABP5 and CRABP2 expression respectively.

2.2. Immunofluorescence

FFPE sections were dewaxed, rehydrated, antigen retrieved in citrate buffer (pH 6, microwave, 20 min), blocked (2% bovine serum albumin, 0.02% fish skin gelatin, 10% fetal bovine serum, 5% goat serum) and incubated with combination of rat FABP5 (MAB3077, R&D Systems, 1:200) and rabbit Cytokeratin (Z0622, Dako, 1:100) or mouse CRABP2 (sc-159,411, SantaCruz Biotechnology, 1:100), and mouse α-SMA (F3777, Sigma-Aldrich, 1:500) overnight (4 °C), followed by 1 h incubation at room temperature with appropriate fluorescent-labelled secondary antibodies (AlexaFluor® 488, 546) and nuclei counterstained with DAPI. Organotypic sections, as previous described [5], were used for positive and negative staining controls. Controls were uniformly negative with appropriate isotype-specific immunoglobulin at matching dilutions.

2.3. Imaging

Immunofluorescent images were taken using the Zeiss Confocal LSM510 microscope at 20× magnification, and images were visualised using Zeiss Zen 2.3 software. The threshold gain and offset was set according to the intensity of the respective channel in the standardizing control organotypic culture sections to eliminate inter-day variability.

2.4. Quantification

Images were quantified using ImageJ software, using a manual method and an automated method. In the manual method, the region of interest was delineated manually using the marker tool in the ImageJ software. Both quiescent PSC (Supplementary Figs. 1 & 2) and activated fibroblasts (Supplementary Figs. 3 & 4) in diseased tissue were quantified. In brief, the quiescent PSC were located next to pancreatic acini, whereas the activated fibroblasts were quantified as clusters within regions of stromal density. For each image, at least six regions of fibroblasts were quantified for their mean FABP5 or CRABP2 intensity, and an average of all six measurements was reported as one data point for that core. Given that up to three cores were quantified per patient, the summary data point for a patient was the median value of up to three cores, or if only one core was available, then this was the summary data point for that patient.

Only FABP5 could be automatically quantified since co-staining with α-SMA allowed identification of fibroblasts in Image-J (supplier) using regions of interest (ROI) function. A threshold was set for measuring high intensity α-SMA regions (green channel), and these ROI were transferred to the FABP5-stained (red) channel. The threshold for α-SMA was kept the same across all cores, and an average was calculated from all the regions measured per core. Similar to the process of manual quantification, the summary data point for each was presented. Quiescent fibroblasts in α-SMA stained tissue could not be quantified for FABP5, as these do not stain positively for α-SMA.

2.5. Comparisons

Comparisons were made using FABP5 and CRABP2 results produced using the manual quantification method. For each patient, a maximum of three cores were measured. The median FABP5 value was matched with the median CRABP2 value for each patient, and these were combined to make a FABP5:CRABP2 ratio. Where there were no matches, due to tissues that were unable to be quantified for either FABP5 or CRABP2, no data point was plotted for that patient.

2.6. Survival curves

For PDAC patients only, the ratio of FABP5:CRABP2 expression was categorized into 3 subsets: high (FABP5:CRABP2 is > 1.2), low (FABP5:CRABP2 is < 0.8) and even (FABP5:CRABP2 is $0.8 < x < 1.2$).

2.7. Statistical analysis

Summary data are expressed as the median with interquartile range as box and whisker (min–max) plots, since the distribution was non-Gaussian. Data were analyzed and FABP5 or CRABP2 expression levels in various tissue types (quiescent fibroblasts vs. activated fibroblasts from a range of diseases) were compared using the Kruskal–Wallis test with Dunn's multiple comparison test (GraphPad Prism, version 8.2). The level of significance was defined as $p < 0.05$. Briefly: $****p < 0.0001$, $***p = 0.0001$ to 0.001, $**p = 0.001$ to 0.01, $*p = 0.01$ to 0.05. Survival comparisons were made between the three subgroups (high, even and low) in a Kaplan-Meier plot. The subgroups were tested for significance using log-rank (Mantel-Cox) test and log-rank test for trend.

To measure the concordance of FABP5/CRABP2 levels across all available cores (up to three cores per patient), the coefficient of variance (CV) was calculated for each patient, where more than one core was quantified (Supplementary Figs. 6–10). CVs greater than 30% were considered very variable, and hence were highlighted on graphs in different colours.

2.8. Western blotting

Cancer cell lysates were loaded at approximately 10 μg. Lysates were separated on 15% SDS-polyacrylamide electrophoresis gels and transferred to nitrocellulose membranes. Membranes were blocked in 5% BSA in 0.1% Tween20-PBS, followed by incubation with primary antibody at 4 °C overnight (FABP5 1:500, CRABP2 1:500 or Hsc-70 1:2000) and then incubation with secondary horseradish peroxidase-conjugated anti-rat, and -mouse antibodies, respectively.

3. Results

3.1. Human ex vivo CAF/PSC expression for CRABP and FABP5

There was a significantly higher CRABP2 intensity (2.5-fold) in quiescent fibroblasts/PSC of normal pancreas (n = 7) as compared to CAF/PSC in PDAC (n = 31, Fig. 1A, Supplementary Figs. 1, 2), mimicked in pancreas of other disease states such as cholangiocarcinoma (CC) and chronic pancreatitis (CP). Similarly, we noted that quiescent fibroblasts/PSC in adjacent normal tissue contained significantly more FABP5 (8-fold) greater than the activated CAF/PSC across almost all diseased tissues, including PDAC, CP and CC (Fig. 1B, Supplementary Figs. 3, 4).

For CRABP2 as well as FABP5 in quiescent fibroblasts, there was a strong concordance between the means of multiple measurements across all three TMA cores for each patient, with coefficient of variations (CVs) calculated across images being under 30% (Supplementary Figs. 5A, 6A). The majority of data plotted for the activated fibroblasts for CRABP2 as well as FABP5 was also highly concordant with a minority of patients with discordant inter-image readings (CV > 30%, Supplementary Figs. 5B, 6B). The patients with discordant results were not the same for FABP5 and CRABP2.

Manually delineating the regions for FABP5 quantification is precise but is time-consuming and may not be reproducible between observers, when performed in a clinical trial setting. We explored a method to quantify FABP5 intensity in a semi-automated fashion. α-SMA stained

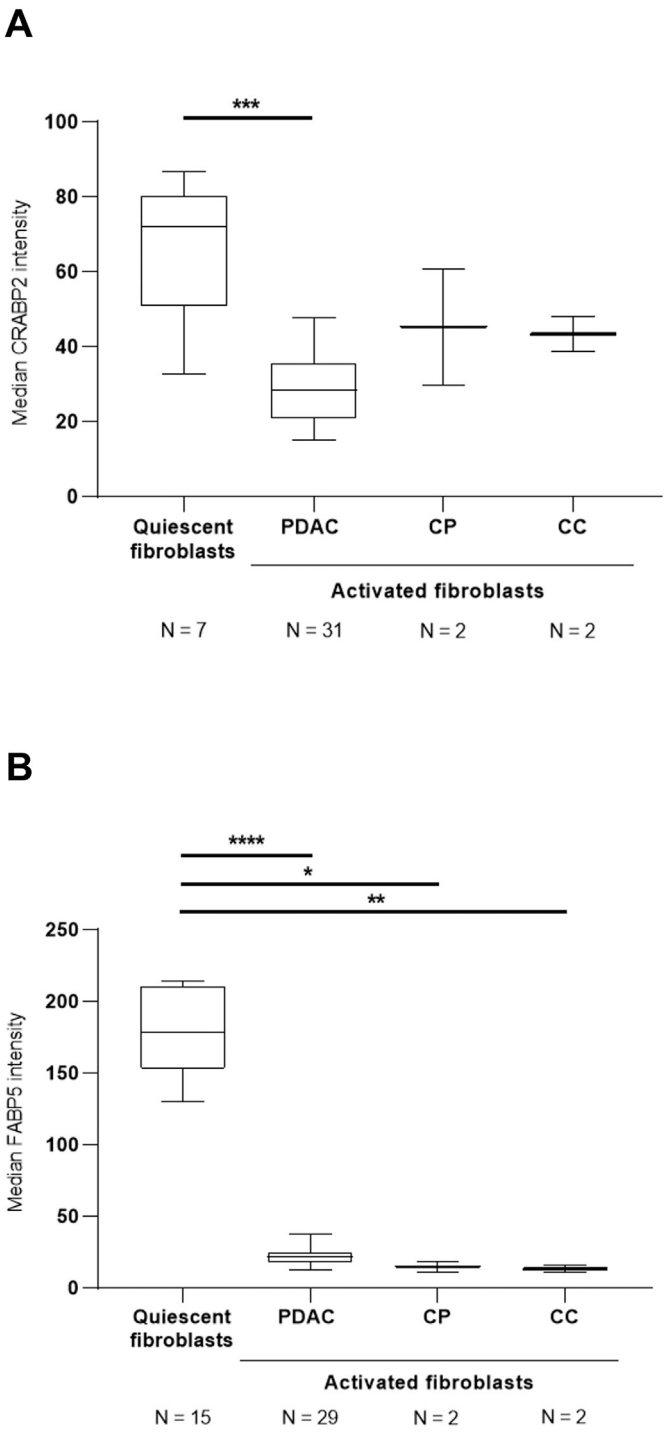

Fig. 1. (A) CRABP2 and (B) FABP5 expression in quiescent and activated PSC. Summary data from immune-fluorescent stained TMA tissue, per patient (N), is depicted as median and interquartile range. CAF/PSC were quantified in a range of tissues: PDAC, CP and CC. Comparisons were made using the Kruskal–Wallis test followed by Dunn's *post-hoc* analysis, ****$p < 0.001$; ***$p < 0.001$; **$p < 0.01$; *$p < 0.05$.

regions were used to quantify the FABP5 in those regions, after images were checked for any artefacts/non-stromal architecture/vasculature and these regions were excluded from the FABP5 measurements. However, this amount of manual input is minimal compared to manually delineating ROI's. Furthermore, we were unable to quantify the FABP5 levels in quiescent fibroblasts/PSC, as these were not positively stained for α-SMA. Therefore, using automated methods, we are

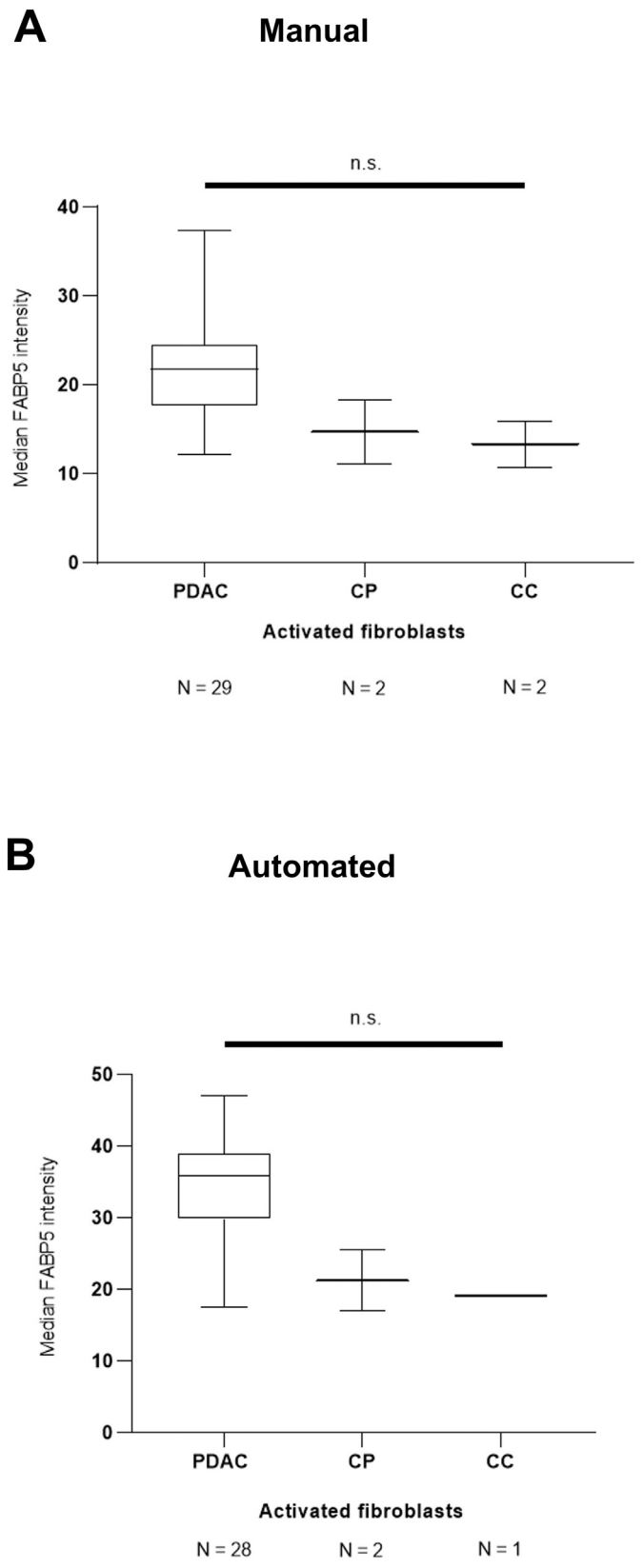

Fig. 2. FABP5 expression in CAF/PSC using (A) manual and (B) automated quantification method. Results from two patients had to be excluded from the automated quantification graph (1 PDAC, 1 CC) because the α-SMA stain was very weak for those corresponding images. n.s. = not significant.

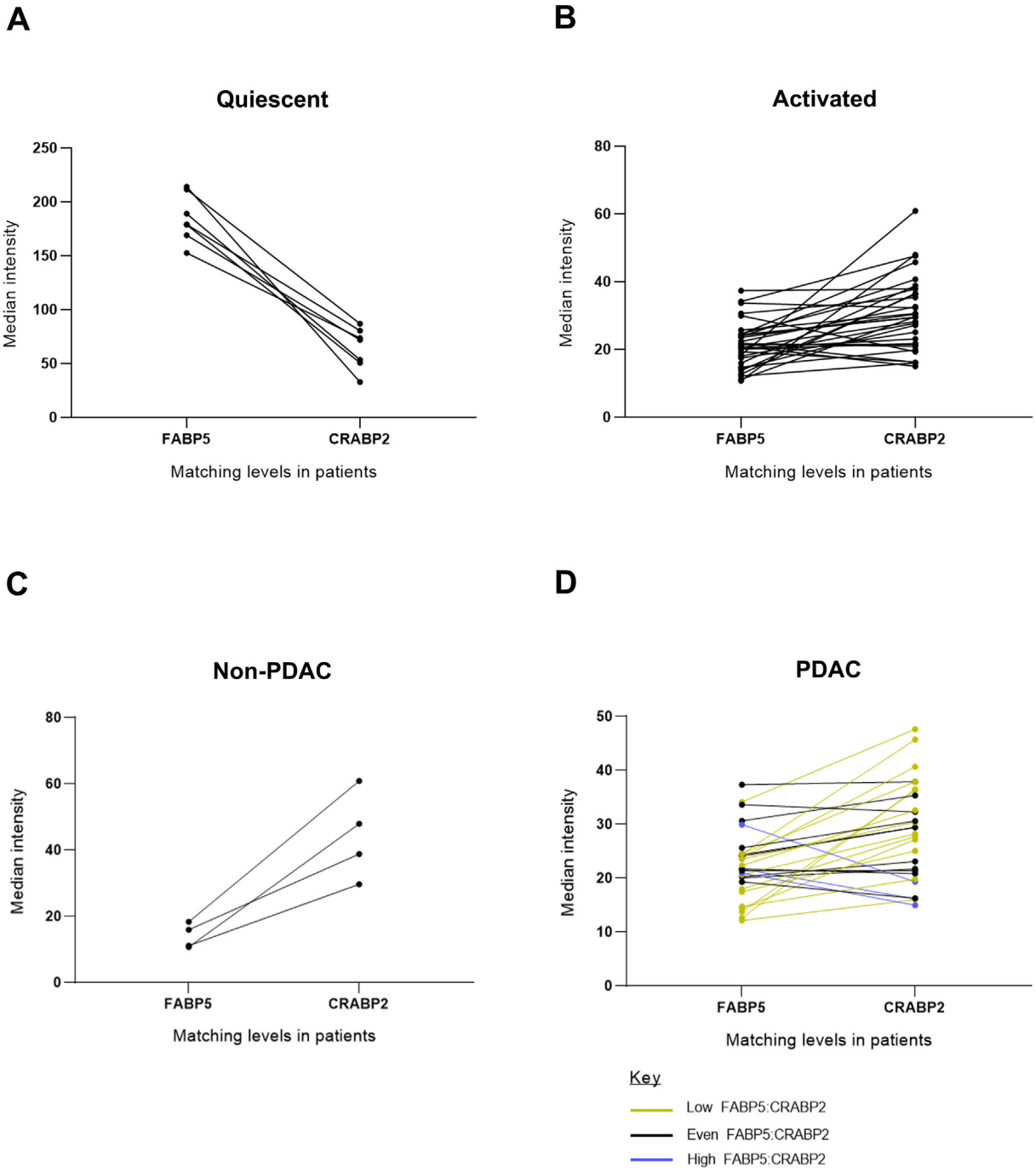

Fig. 3. Correlating FABP5 and CRABP2 levels in quiescent (A) and activated (B) PSC/CAF in matched TMA cores of respective patients. Further assessment of (C) non-PDAC tissues (N = 4, CP = 2, CC = 2) and (D) PDAC tissue (N = 28). For PDAC patients only, the ratio of FABP5:CRABP2 expression was categorized into 3 subsets: high (FABP5:CRABP2 is > 1.2, blue), low (FABP5:CRABP2 is < 0.8, yellow) and intermediate (FABP5:CRABP2 is 0.8–1.2, black). (For interpretation of the references to colour in this figure legend, the reader is referred to the web version of this article.)

only able to compare the levels of FABP5 among CAF/PSC in diseased tissues (Fig. 2, Supplementary Fig. 7). The CAF/PSC FABP5 levels were highly concordant (Supplementary Fig. 8). Thus, semi-automated quantification can be used in future biomarker analyses.

Next we compared each patient's matched FABP5:CRABP2 levels in quiescent PSC from (Fig. 3A). The quiescent PSC consistently show a pattern of high FABP5:CRABP2 ratio, ranging from 2:1 to 7:1. There was a lot more variability in the FABP5:CRABP2 ratios of the activated CAF/PSC (Fig. 3B). For non-PDAC patients (CP and CC), all tissues showed a low FABP5:CRABP2 ratio (between 0.2:1 and 0.4:1, Fig. 3C). In particular, this variability was more pronounced in PDAC tissues (Fig. 3D). The ratio of FABP5:CRABP2 expression could potentially be categorized into 3 subsets: high (FABP5:CRABP2 is > 1.2, 10.7%, 3 patients), low (FABP5:CRABP2 is < 0.8, 50%, 14 patients) and even (FABP5:CRABP2 is 0.8–1.2, 39.3%, 11 patients).

3.2. Human ex vivo epithelial expression for CRABP2 and FABP5

There was a significantly higher (2-fold) CRABP2 intensity in normal epithelial cells versus PDAC epithelial cells, mimicked in pancreas of patients with other disease states such as CP and CC (Fig. 4A), with a similar range of variance and a high level of concordance

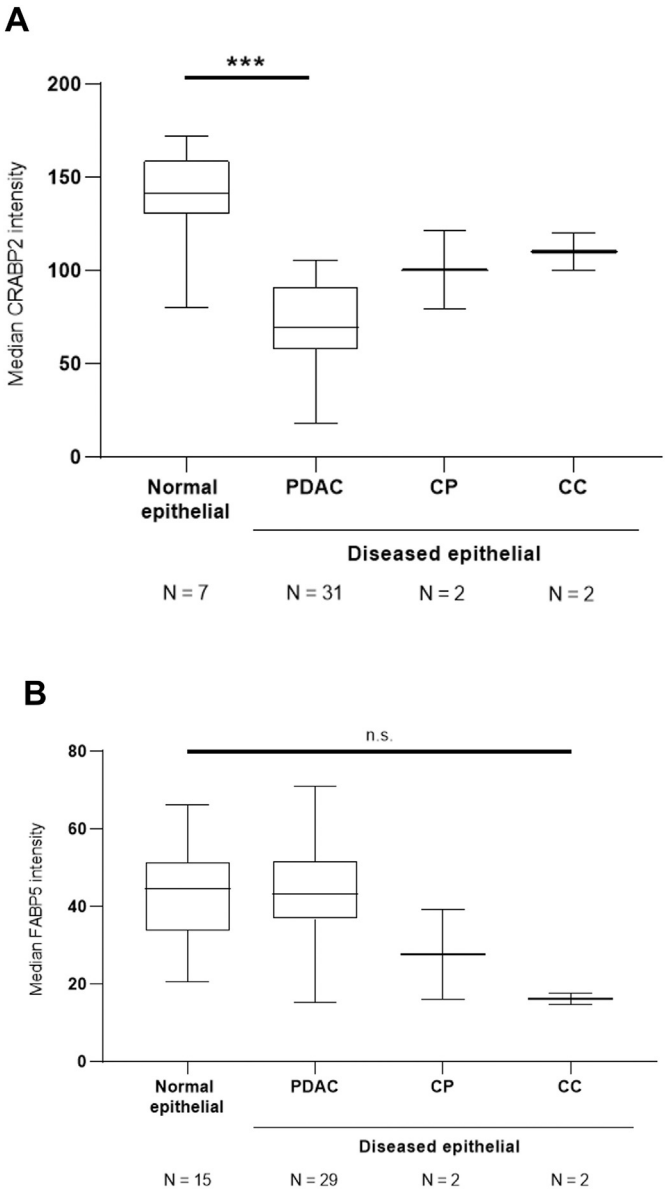

Fig. 4. (A) CRABP2 and (B) FABP5 expression in the normal and diseased epithelial cells from a range of pancreatic tissues: PDAC, CP and CC. Summary data from immune-fluorescent stained TMA tissue, per patient, is depicted as median and interquartile range. Comparisons were made using the Kruskal–Wallis test followed by Dunn's *post-hoc* analysis, ***$p < 0.001$; n.s. = not significant.

(CV < 30%) on repeated measures for each patient (Supplementary Fig. 9). In contrast, the FABP5 expression in PDAC epithelial cells matched that of the normal epithelial cells, (Fig. 4b), but also, with a similar range of variance and a high level of concordance (CV < 30%) on repeated measures for each patient (Supplementary Fig. 10).

Consistent with the pattern found for quiescent PSC the normal epithelial regions consistently reveal a high FABP5:CRABP2 ratio (range: 2.6 to 3.3:1), in all 7 patients measured (Fig. 5A). There was greater variability in the FABP5:CRABP2 ratios of the epithelial cells across all diseased tissues, when compared to that of normal epithelial cells (Fig. 5B). In particular, and similar to that of fibroblast, this variability was more pronounced in PDAC-specific tissues, compared to non-PDAC tissues (CP and CC, Fig. 5C–D). Similar to CAF/PSC, the ratio of FABP5:CRABP2 expression for epithelial regions of PDAC patients only, could be categorized into 3 subsets: high (FABP5:CRABP2 is > 1.2, 1 patient), low (FABP5:CRABP2 is < 0.8, 75%, 21 patients) and even (FABP5:CRABP2 is 0.8–1.2, 21.4%, 6 patients). There was no statistically significant difference between these ratio subgroups for CAF or epithelial cells, when survival data was examined (Fig. 6A–B), although it appeared that the low ratio subgroups, in epithelial cells, had a more favorable prognosis. In addition, there was a more favorable range of tumor stages (T1 – T3) in patients with a low ratio, compared to those with an even ratio (T2 - T3), which had a greater abundance of Stage 3 tumors (Supplementary Fig. 11). There were more patients with R1 resections in the low ratio group, when compared to the even ratio group (Supplementary Fig. 12). However, this dataset had too few patients in each sub-group to reach any robust conclusions.

FABP5 and CRABP2 proteins were present in normal stellate cell (PS1), and some cancer cell (Aspc1 and Patu-S) lysates, but not in Capan-1 (Fig. 7).

4. Discussion

ATRA is particularly effective in treating promyelocytic leukemia (PML), where it exerts its effects via binding to the retinoic acid receptor (RAR) targeting abnormal fusion protein PML-RARA due to chromosomal translocation [6]. RAR has been known to regulate the expression of numerous target genes involved in cell-cycle control, differentiation and apoptosis [7]. It limits cell growth and has anti-carcinogenic effects. As CRABP2 facilitates the transport of retinoic acid (RA) to RAR, it is key in orchestrating these effects [8].

However, despite the seemingly tumor suppressive effects of retinoids, it has been hypothesized that they can sometimes have pro-carcinogenic effects. This was seen when a lung cancer chemoprevention trial (CARET), assessing the efficacy and safety of beta-carotene and retinol, was prematurely terminated as the treatment apparently increased the incidence of the cancer [9]. It is postulated that this effect was mediated by the alternate nuclear ligand/receptor for retinoic acid: PPARβ/δ [10]. Indeed, this ligand-dependent nuclear receptor targets genes that enhance cell survival and proliferation [11], thereby associating it with pro-carcinogenic characteristics. In addition to this, RA is transported to PPARβ/δ by FABP5. Given that RA can be translocated by either CRABP5 or FABP5, to different nuclear receptors which in turn control transcription of target genes of opposing effects, it is postulated that an imbalance in the ratio of these RA-binding proteins may govern which effects are more prominent [12]. With this in mind, it is useful to highlight that there is a greater binding affinity of RA to the CRABP2-RAR pathway [13,14], than that of the FABP5-PPARβ/δ pathway [15]. Therefore RA signalling seems to occur mainly through RAR binding (via CRABP2), unless there is a high FABP5/CRABP2 ratio [16].

It has been suggested that FABP5 levels can be used as a prognostic biomarker for survival in breast cancer [17]. According to Liu, RZ. et al, there was a correlation between FABP5 levels and tumor growth response to RA. FABP5 is also significantly overexpressed in intrahepatic cholangiocarcinoma (IHCC) with lymph node metastasis and is involved in cell proliferation and invasion in vitro. It was therefore suggested that FABP5 is associated with tumor progression in ICC [18]. Furthermore, a high FABP5 to CRABP2 expression ratio may be related to craniopharyngiomas tumor recurrence, with ATRA demonstrating beneficial effect [19]. Hence, we anticipated that FABP5 would have a greater expression in diseased tissue, versus normal adjacent tissue.

FABP5 and CRAPB2 are expressed in patient-derived PDAC cell lines, and response to ATRA was observed to be dependent upon differential expression of FABP5 versus CRABP2 [20]. Elevated FABP5 expression was associated with minimal cytotoxicity and tumor growth inhibition, and a complementary increase in migration and invasion. CRABP2 expression in the absence of FABP5 was associated with significant tumor growth inhibition with ATRA, even in gemcitabine-resistant tumors. Furthermore, the ATRA-resistant phenotype of FABP5^{high}CRABP2^{null} cells could be overcome by ectopic expression of CRABP2. This encouraged us to investigate the levels of FABP5 and

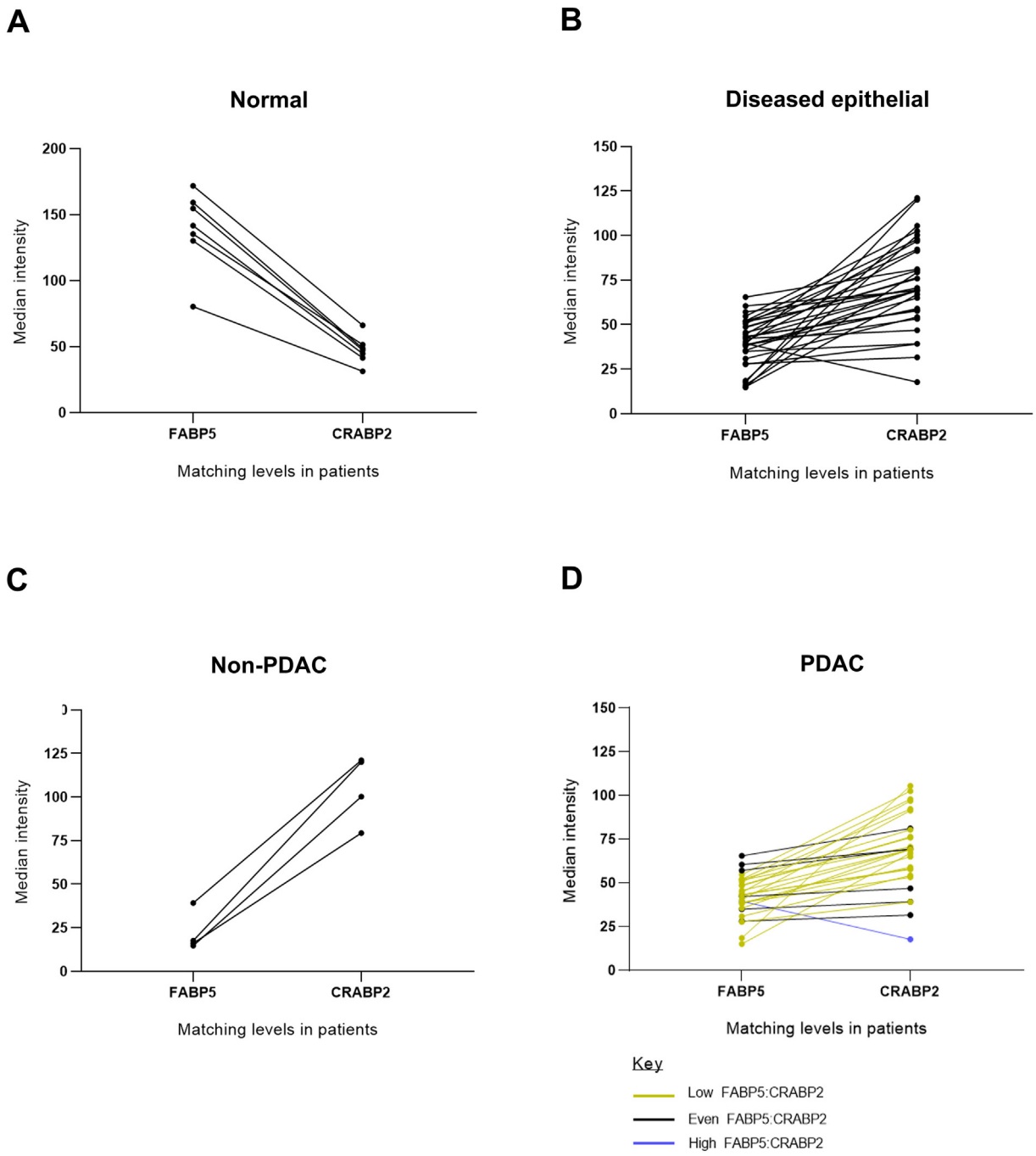

Fig. 5. Correlating FABP5 and CRABP2 levels in normal (A) and diseased epithelial (B) cells in matched TMA cores of respective patients. Further assessment of (C) non-PDAC tissues (N = 4, CP = 2, CC = 2) and (D) PDAC tissue (N = 28). For PDAC patients only, the ratio of FABP5:CRABP2 expression was categorized into 3 subsets: high (FABP5:CRABP2 is > 1.2, blue), low (FABP5:CRABP2 is < 0.8, yellow) and intermediate (FABP5:CRABP2 is 0.8–1.2, black). (For interpretation of the references to colour in this figure legend, the reader is referred to the web version of this article.)

CRABP2 in fibroblasts, as well as epithelial cells.

In this study, we demonstrate that there is a significantly lower CRABP2 and FABP5 intensity in activated PSC, versus quiescent fibroblasts. Furthermore, quiescent fibroblasts had a consistently high FABP5:CRABP2 ratio, whereas all non-PDAC tissue PSC showed a low FABP5:CRABP2 ratio, and PDAC PSC had a range of FABP5:CRABP2 ratios (high, even and low). We postulate that fibroblasts might affect the pathogenesis in an asymmetric fashion to epithelial cells, where quiescent fibroblasts can exhibit a high FABP5:CRABP2 ratio, which is not pro-tumorigenic, but instead, tumor suppressive. A larger cohort for studying outcome of patients with a high FABP5:CRABP2 ratio is required, particularly in a clinical trial context where patients are treated with ATRA. Furthermore, it appears that CRABP2 may play a bigger role than FABP5 in epithelial cells and may reflect the disease status such as tumor size.

We also demonstrate that automated quantification can be used as a valid substitute for manual quantification in future biomarker analysis, which not only saves time, but also excludes the possibility of operator bias, without compromising on accuracy.

A

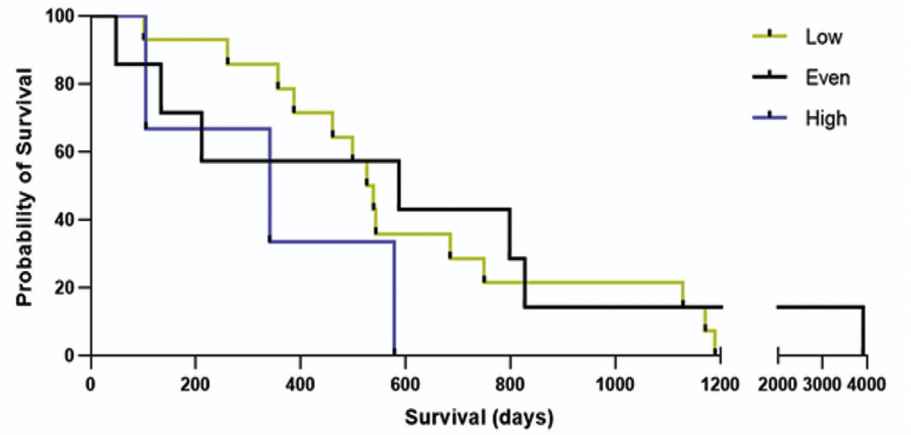

	Patient surviving (patient dead)								
Day:	0	200	400	600	800	1000	1200		4000
High	3 (0)	2 (1)	1 (2)	0 (3)	0 (3)	0 (3)	0 (3)		0 (3)
Even	11 (0)	7 (2)**	6 (3)	4 (4)*	3 (5)	1 (6)*	1 (6)		1 (6)
Low	14 (0)	13 (1)	10 (4)	5 (9)	3 (11)	3 (11)	0 (14)		0 (14)

B

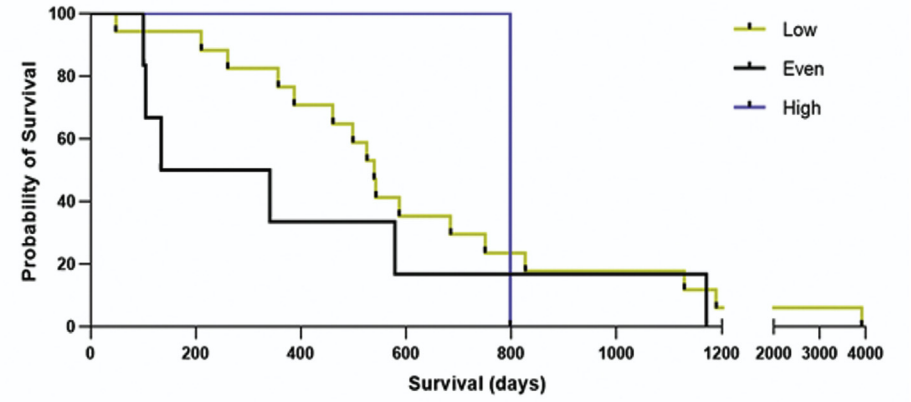

	Patient surviving (patient dead)								
Day:	0	200	400	600	800	1000	1200		4000
High	1 (0)	1 (0)	1 (0)	1 (0)	0 (1)	0 (1)	0 (1)		0 (1)
Even	6 (0)	3 (3)	2 (4)	1 (5)	1 (5)	1 (5)	0 (6)		0 (6)
Low	21 (0)	18 (1)**	14 (5)	7 (11)*	5 (13)	3 (14)*	1 (16)		0 (17)

Fig. 6. Kaplan-Meier survival comparisons between patients with high (FABP5:CRABP2 is > 1.2), low (FABP5:CRABP2 is < 0.8) and even (FABP5:CRABP2 is 0.8–1.2) expression ratios measured in CAF/PSC (A) and epithelial cells (B). Tests for significance included log-rank (Mantel-Cox) test and log-rank test for trend. Yellow boxes highlight when patients have been lost to follow-up. *denotes number of patients lost to follow-up. (For interpretation of the references to colour in this figure legend, the reader is referred to the web version of this article.)

Declaration of competing interest

The authors declare that there is no conflict of interest.

Acknowledgements

We thank the technicians from Core Facilities (Pathology, Microscopy), members of Kocher laboratory for insightful critical comments. This work was supported by core centre grant from Cancer Research UK (C16420/A18066). Contributions included designing research studies (CSH, HMK), conducting experiments (CSH), analyzing data (CSH, HMK), providing reagents/insight (JCA, HMK), and writing the manuscript (all authors).

Appendix A. Supplementary data

Supplementary information is available at Laboratory Investigation's website. Supplementary data to this article can be found

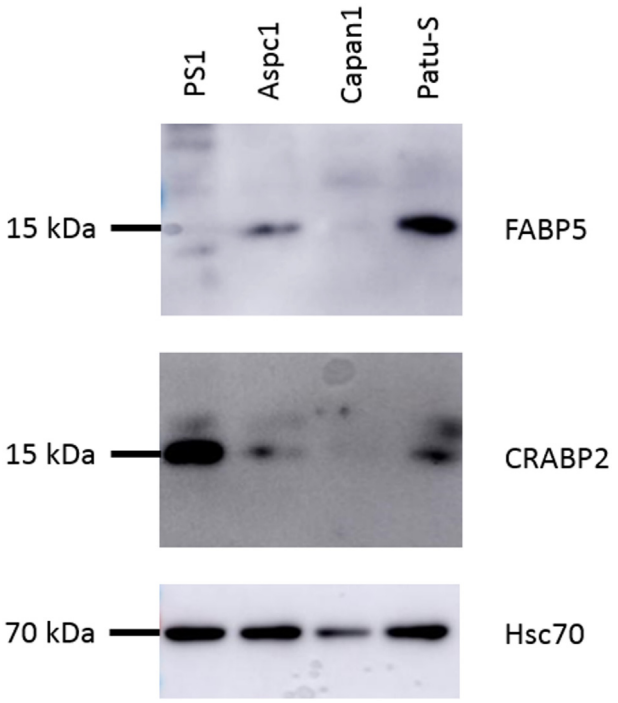

Fig. 7. Western blots showing expression of FABP5 and CRABP2 in cancer and PS1 cell lysates.

online at https://doi.org/10.1016/j.anndiagpath.2020.151557.

References

[1] Froeling FE, Kocher HM. Homeostatic restoration of desmoplastic stroma rather than its ablation slows pancreatic cancer progression. Gastroenterology 2015;148:849–50.
[2] Carapuca EF, Gemenetzidis E, Feig C, Bapiro TE, Williams MD, Wilson AS, et al. Anti-stromal treatment together with chemotherapy targets multiple signalling pathways in pancreatic adenocarcinoma. J Pathol 2016;239:286–96.
[3] Schug TT, Berry DC, Shaw NS, Travis SN, Noy N. Opposing effects of retinoic acid on cell growth result from alternate activation of two different nuclear receptors. Cell 2007;129:723–33.
[4] Froeling FE, Mirza TA, Feakins RM, Seedhar A, Elia G, Hart IR, et al. Organotypic culture model of pancreatic cancer demonstrates that stromal cells modulate E-cadherin, beta-catenin, and Ezrin expression in tumor cells. Am J Pathol 2009;175:636–48.
[5] Arumugam P, Bhattacharya S, Chin-Aleong J, Capaso M, Kocher HM. Expression of polymeric immunoglobulin receptor and stromal activity in pancreatic ductal adenocarcinoma. Pancreatology 2017;17:295–302.
[6] de The H, Chomienne C, Lanotte M, Degos L, Dejean A. The t(15;17) translocation of acute promyelocytic leukaemia fuses the retinoic acid receptor alpha gene to a novel transcribed locus. Nature 1990;347:558–61.
[7] di Masi A, Leboffe L, De Marinis E, Pagano F, Cicconi L, Rochette-Egly C, et al. Retinoic acid receptors: from molecular mechanisms to cancer therapy. Mol Aspects Med 2015;41:1–115.
[8] Donato LJ, Noy N. Suppression of mammary carcinoma growth by retinoic acid: proapoptotic genes are targets for retinoic acid receptor and cellular retinoic acid-binding protein II signaling. Cancer Res 2005;65:8193–9.
[9] Omenn GS, Goodman GE, Thornquist MD, Balmes J, Cullen MR, Glass A, et al. Effects of a combination of beta carotene and vitamin A on lung cancer and cardiovascular disease. N Engl J Med 1996;334:1150–5.
[10] Shaw N, Elholm M, Noy N. Retinoic acid is a high affinity selective ligand for the peroxisome proliferator-activated receptor beta/delta. J Biol Chem 2003;278:41589–92.
[11] Wang D, Wang H, Guo Y, Ning W, Katkuri S, Wahli W, et al. Crosstalk between peroxisome proliferator-activated receptor delta and VEGF stimulates cancer progression. Proc Natl Acad Sci U S A 2006;103:19069–74.
[12] Schug TT, Berry DC, Toshkov IA, Cheng L, Nikitin AY, Noy N. Overcoming retinoic acid-resistance of mammary carcinomas by diverting retinoic acid from PPARbeta/delta to RAR. Proc Natl Acad Sci U S A 2008;105:7546–51.
[13] Dong D, Ruuska SE, Levinthal DJ, Noy N. Distinct roles for cellular retinoic acid-binding proteins I and II in regulating signaling by retinoic acid. J Biol Chem 1999;274:23695–8.
[14] Sussman F, de Lera AR. Ligand recognition by RAR and RXR receptors: binding and selectivity. J Med Chem 2005;48:6212–9.
[15] Tan NS, Shaw NS, Vinckenbosch N, Liu P, Yasmin R, Desvergne B, et al. Selective cooperation between fatty acid binding proteins and peroxisome proliferator-activated receptors in regulating transcription. Mol Cell Biol 2002;22:5114–27.
[16] Schug TT, Berry DC, Shaw NS, Travis SN, Noy N. Dual transcriptional activities underlie opposing effects of retinoic acid on cell survival. Cell 2007;129:723–33.
[17] Liu RZ, Graham K, Glubrecht DD, Germain DR, Mackey JR, Godbout R. Association of FABP5 expression with poor survival in triple-negative breast cancer: implication for retinoic acid therapy. Am J Pathol 2011;178:997–1008.
[18] Jeong CY, Hah YS, Cho BI, Lee SM, Joo YT, Jung EJ, et al. Fatty acid-binding protein 5 promotes cell proliferation and invasion in human intrahepatic cholangiocarcinoma. Oncol Rep 2012;28:1283–92.
[19] Li Q, You C, Zhou L, Sima X, Liu Z, Liu H, et al. All-trans retinoic acid inhibits craniopharyngioma cell growth: study on an explant cell model. J Neurooncol 2013;112:355–64.
[20] Gupta S, Pramanik D, Mukherjee R, Campbell NR, Elumalai S, de Wilde RF, et al. Molecular determinants of retinoic acid sensitivity in pancreatic cancer. Clin Cancer Res 2012;18:280–9.